

Surface Modification of SS410 and SS316L Medical Implants through Nitriding and Boriding Coatings: Advancing Biocompatibility and Performance

Ilaiyavel Sivakumaran¹, Harish Ramanathan Babu², Atul SC³

{ilaiyavel@svce.ac.in¹, harishramanathan74@gmail.com², atulsc12@gmail.com³}

Dept of Mechanical Engineering, Sri Venkateswara College of Engineering, Sriperumbudur, Tamilnadu.^{1,2}, Diffuson Coatech, Chennai, Tamilnadu³

Abstract. Titanium and stainless steel alloys, for example, are essential components of modern medicine and play a vital role in the medical business. A number of titanium alloys, including AISI 410 and AISI 316L, and stainless steel materials have been selected for usage in the medical business due to their widespread availability and extensive use. The objective of this research is to look at the microbiological and tribological characteristics of the materials listed above that have undergone various controlled treatments, such as surface treatment of the alloys using thermal diffusion. Thermal diffusion treatments known commercially as boronizing and nitriding were utilized. All of the base materials had their surface hardness and wear resistance increased by both nitriding and boronizing treatments. The boriding treatment resulted in a significant increase in surface roughness, but it also maximized surface hardness and reduced wear losses. Both nitriding and boronizing processes produced antibacterial activity against *subtilis bacillus* bacterial

Keywords: Medical implant, Coating, nitriding, boronizing.

1 Introduction

Over the last several decades, medical science has greatly improved thereby increasing the lifespan of humans. As people age their loadbearing joints become more prone to ailments, this in turn, led to a rapidly increasing number of surgical procedures involving prosthesis implantation [1]. Today more than 12 grades of titanium have been made available; these grades are divided into 2 generations. Alloys from 1950-1990 are termed as first-generation alloys and alloys from 1990 until present are classified as second-generation titanium alloys. Ti6Al4V [1st Generation] is one of the most commonly used titanium alloys, originally developed for aerospace applications, it has found its way into medical industry replacing commercially pure titanium in the joint replacement segment owing to its better resistance to wear and improved fatigue life. The Ni-Ti SMA material is characterized by its good biological, MRI and computer tomography compatibility [2]. The properties of SMA

materials such as PE and SME have been greatly exploited in the delicate areas of dentistry, vascular, neurological, etc. applications [3]. Nitriding is the process of implanting nitrogen atoms into the surface of the substrate to form hard metal nitrides to combat wear and improve corrosion in some cases [4,5]. The effect of nitriding in improving the wear resistance of load-bearing joint replacement implants has been effectively studied [6,7,8]. Some researchers have also explored the use of nitriding in enhancing the functionality of stents [9]. Implants similar to stents, catheters, guide wires, etc., need to possess a low coefficient of friction in order to slide into a human body with the least effort and sensation [10,11]. Coatings of polymers like PTFE [Polytetrafluoroethylene], PEEK [Polyether ether ketone], etc., in the cases like the joint replacement surgeries, UHMWPE [ultra-heavy molecular weight polyethylene] are used to additionally damp the load acting on the joint socket [12,13]. The use of antibiotics for the treatment of infection associated with implanted devices has been the industry standard for several decades [14]. The use of antibiotic-infused implants for preventing or suppressing infection associated with implants has been common [15]. However, selecting the right antibiotic to infuse in the implant can be very difficult due to the range of bacteria that could be present in the implant site [16]. The onset and rate of release of antibiotics are difficult to control and can induce antibiotic resistance. The bacteria and the patient may develop sensitivity to the antibiotic [17,18]. Functionalizing of implant surface by modifying the chemistry, morphology has emerged as an important area of research [19]. Nano textured surfaces are being explored in hopes to produce bactericidal surfaces for the mechanical contact killing of pathogens [20]. The objective of this research is to enhance the surface qualities of materials used in the manufacturing of medical implants namely stainless steel and titanium. Producing the desired surface modifications by thermal diffusion coating technology and improving the bactericidal properties of specimen materials against *subtilis bacillus*.

2 Experimental Procedure

The elemental composition of the material has been displayed in the table.1 below as weight percentage of elements.

Table 1. Chemical composition of the stainless steel used determined by X-Ray fluorescence (%Wt.)

	c	cr	Ni	Mo	Si	Mn	Fe
SS410 Martensitic Stainless steel	0.15	12.51	0.76	0.04	0.54	1.0	85
SS316L Austenitic stainless steel	0.01	18	12.8	2.4	0.23	0.5	66.06

Specimens in wide variety of geometries and dimensions were prepared for the tribological and metallurgical characterization. Prescribed guidelines and procedure were following during the machining of specimens from parent stock. For example, ASTM G99 and G65 Standard guidelines for specimen preparation for pin on disc test and abrasive wear tests were followed. Well established machining procedures like turning and milling were used in manufacturing the specimens.

2.1 Nitriding Process

The nitriding salt was filled in the nitriding retort and melted at a temperature of 525 °C. once all the salt was melted, the temperature was raised to set nitriding temperature of 570 °C and held there for a duration of 10 hours. The washed and dried specimens were stacked in a nitridation jig fabricated using mild steel. The jig was submerged along with its content into the nitriding retort and held for a predetermined duration and later water cooled. Possible reactions taking place during nitridation treatment is given below in the equation. Ammonia in the presence of heat and catalyst breaks down and liberates nitrogen ions and hydrogen molecules. The nascent ions of nitrogen dissolve in alpha iron during nitriding treatment. Sometimes this hydrogen generated is also adsorbed into the surface of the metal. The diffused nitrogen ions chemically combine with the nitride-forming element in the substrate such as iron, chromium, etc. through a catalytic reaction.



Table 2. Nitriding treatment parameters

Parameter	Level
Temperature	560 °C
Duration	120 minutes
Pressure	Atmospheric pressure
Post-processing	Water cooling

2.2 Boride Diffusion Coating

During the preparation of furnace for boronizing process, the SS 435 retort was removed and one of the coil temperatures measuring thermocouple was disconnected since the boronizing enclosure only occupied half the height of the furnace. An inverted graphite crucible was placed on the bottom of the furnace to elevate the boronizing enclosure. The boronizing reactor was fabricated using a pipe of Ø32 mm (ID) with provision to accept the machined temperature probe from the behind. The reaction container for boronizing was made airtight so as to prevent escaping of active boron elements. The specimens were washed cleaned and wiped with acetone to prevent any contamination. The clean specimens were leaded into the SS 310 chamber and was preheated to 300 °C and subsequently 700 °C to prevent thermal shocking in the pre-descried muffle furnace. The machined temperature probe was inserted into the SS chamber in the hot condition and was gently placed inside the furnace preheated to 920 °C for undergoing thermal diffusion processes.

Table 3. Boronizing treatment parameters

Parameter	Level
Temperature	900 °C
Duration	120 minutes
Pressure	Atmospheric pressure
Post-processing	Normalizing

2.3 Tribological test:

Dry sand abrasion wear characterization were conducted using a test rig designed and built in house based on ASTM G65 standard. The parameters used during the dry sand abrasive wear investigations and the schematic of the abrasive wear testing machine is represented in the Table 4 and Figure 1 respectively. Wear loss occurring during the open three body wear testing period is reported in the form of mass loss by weighing the specimens before and after abrasion testing. The weight of the specimens was measured using a calibrated electronic weighing scale with 0.5 g least count ± 0.001 g accuracy. The working of the abrasion wear test rig can be observed from the schematic provided in the figure. In addition to reporting the weight lost due to the abrasion wear testing the depth of the wear scar is also reported in this research.

Table 4. Boronizing treatment parameters

Description	Specification
Specimen dimensions	75 × 25 × 12.4 mm
Abrasive media	Silica
Particle size	120–180 mesh
Force	90 N
Duration	25 minutes
Speed	240 rpm
Wheel diameter	230 mm
Backing material	Butyl rubber wheel
Temperature	29 °C

The rotating disc used in the pin on disc test rig was AISI 440C martensitic stainless steel material, CNC turned to Ø165 mm and ground to mirror finish on a flood cooled surface grinder. The machined disc was subjected to heat treat using standard heat treatment practice recommended by SAE and tempered at 230 °C in a conventional electrical resistance furnace.

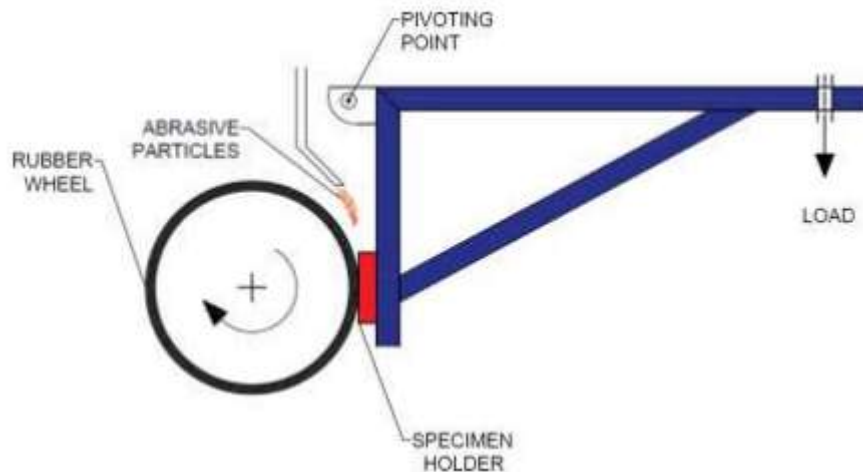


Fig. 1. Schematics for abrasive wear tester based on ASTM G65 standard

2.4 Micro Biological Investigation

Bacterial sensitivity of the surface is an important characteristic of a bio-material. Bacterial sensitivity of the material can determine how the doctors could use the material to better treat a patient. Therefore, the surface of the material was examined for its bacterial sensitivity characteristics. *Bacillus subtilis*, a gram-positive bacterium, commonly used in laboratories as a model organism was used to investigate the bacterial adhesion and bactericidal activities that the surface modified material may display. The tests were conducted in-vitro, specifically in Ø90 mm petri dishes. Bacteria from frozen reserve was revived in sterilized nutrient broth at 35 °C shaking at 150 rpm for 24 hours. The bacterial sensitivity tests were planned to be conducted in two formats. All dishes used in the experiment were washed following standard operating procedure. Nutrient agar for culturing the bacteria was prepared by dissolving the nutrient powders in reverse osmosis treated water at neutral water PH 28°C in a sterile conical flask. All petri dish sets, swabs, surface modified and untreated specimens were all subjected to autoclave-sterilization. in a process graphically represented in the figure below. All the experiments involving the bacteria were performed in laminar air flow chamber following standard laboratory procedure. The bottom surface of the laminar air flow hood was first wiped with rubbing alcohol and then exposed to UV light for 5 minutes to sterilize the hood. Required number of petri dishes were taken from sterile storage and unwrapped their aluminum foil covers. Specimen control plates were prepared by pouring 20 ± 1 ml of prepared solutions. The first plate was plain nutrient agar with no traces of bacteria. The second plate plain nutrient agar with bacterial broth spread on the surface using cotton swab; this technique is to be hence forth termed as poured & swabbed. The third plate was agar and broth swirl-mixed at 1:3 :: broth : agar ratio and poured into the plate; this technique is to be hence forth called as swirled & poured plate. The photographs of the specimen control plates are displayed in Figure below. All the plates were carefully closed in the laminar air flow chamber and placed into the incubation chamber set to 37 ± 2 °C.

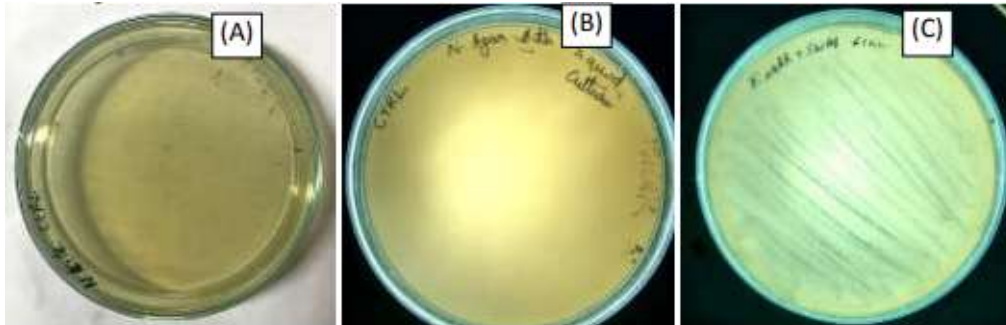


Fig. 2.Control plates used in microbiological investigations for bacterial sensitivity.[A] Nutrient agar, [B] Nutrient agar with liquid culture and [C] Nutrient agar with swabbed culture

3 Results and Discussion

3.1 Surface Morphology

As expected, the method of manufacturing the specimen played a curtail role on surface finish and rough of the specimen. Additional polishing the specimens with diamond paste reduced the roughness when measured using tactile profilometer. When the specimens subjected to diamond polishing post thermal diffusion treatments, the reduction in roughness were of greater magnitude. The specimens subjected to polishing post boronizing reported the least roughness values. The machined specimens (milled) consistently reported roughness values at $2.16 \pm 0.2 \mu\text{m}$. A maximum roughness reduction of 450% was observed in borided austenitic stainless steel specimen. An average roughness of $0.64 \mu\text{m Ra}$ was reported on the post polished specimens. The following graph displays the influence of manufacturing processes on the surface rough and effect of polishing post-treatment for thermally diffused specimens on surface finish.

The specimens subjected to nitriding displayed the least change in roughness values. A significant increase in roughness from the base line values were observed in boron diffused specimens. This is considered to be caused due to the relatively higher temperature involved in the boronizing process. Multiple yester studies have been conducted linking the process temperature and increment in surface roughness value. The author considers there exists a relationship between the method of boron diffusion technique and surface roughness. Post diffusion heat treatment greatly affected the polished specimens compared to as machined specimens.

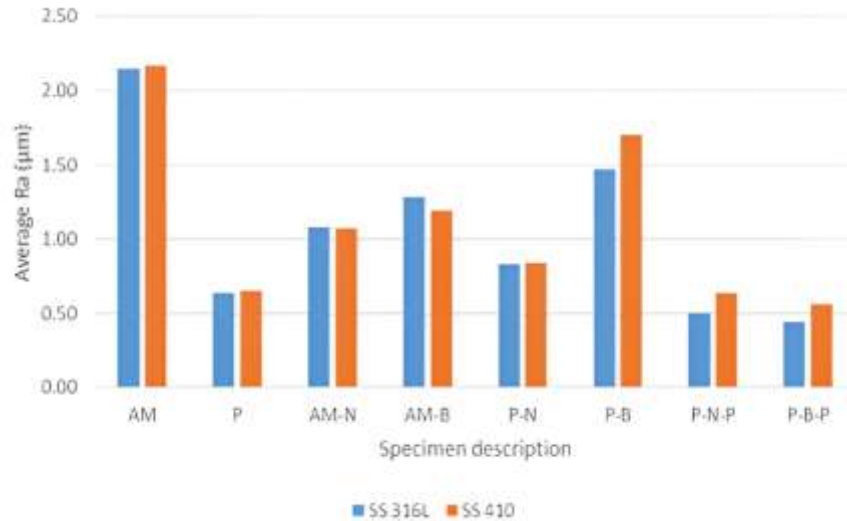


Fig. 3. Graphical representation of surface roughness measured using tactile profilometer

Table 4. Explanation for symbols and abbreviations used in Figure 3

Abbreviation	Explanation	Abbreviation	Explanation
AM	As Machined specimen	P-N	Polished specimen nitride
P	Polished specimen	P-B	Polished specimen borided
AM-N	Nitrided as machined specimen	P-N-P	Polished nitrided and polished specimen
AM-B	Borided as machined specimen	P-B-P	Polished borided and polished specimen

3.2 Surface Hardness

Micro Vickers hardness tester was used to measure the traverse and surface hardness.. The hardness profile was plotted based on the observations made on various specimens. The surface hardness of the treated specimens was vastly higher than the unprocessed specimens. The influence of surface preparation techniques on the surface and traverse hardness of the thermally diffused specimens were minimal. A maximum surface hardness of 1241 HV0.1 was observed on the nitrided austenitic stainless steel (316L) specimens and a slightly lower surface hardness of 1014 HV0.1 was observed on the nitrided martensitic stainless steel AISI

410. The increase in surface hardness provided by the thermal diffusion treatments is up to 4.8 times higher than soft materials. The hardness of the unprocessed materials was recorded at 223 HV0.1, 157 HV0.1 and 144 HV0.1 for SS410, SS316L and CP Ti respectively.

The increase in the hardness value of the thermally diffused specimen is caused due to the diffusion of boron and nitrogen into the surface of the test specimens. The diffusion of boron has caused the formation of metal borides like diiron borides and chromium borides in SS316L and SS410. In the case of nitriding treatment, similar to boronizing, hard compound layer was observed in addition to a relatively softer diffusion layer. The rate of diffusion during both nitriding and boronizing was much slower compared to the ferrous alloys. Due to this reason, a rapid fall in the hardness was observed in the hardness profile mapping.

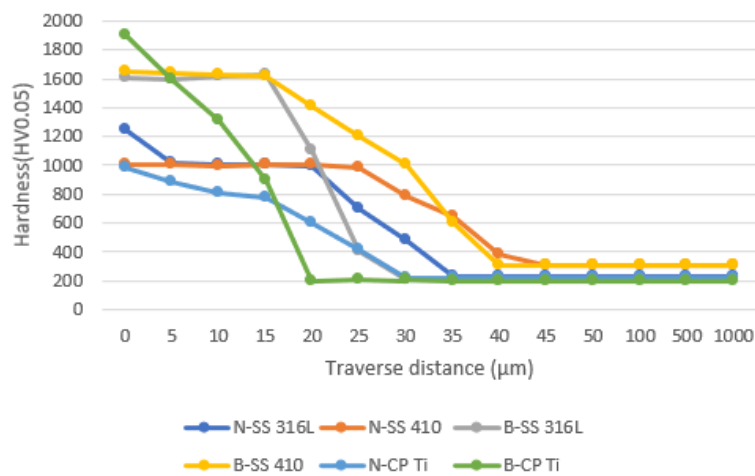


Fig. 4. Hardness profile mapped using traverse hardness measuring technique

3.3 Dimensional Variation Analysis

In addition to being able to produce required roughness repeatedly, the dimensions of the medical implants are also critical for some parts like stents, surgical shears, parts of assembly etc. where fits and tolerance would have to be met to produce successful assembly. In this research the change in dimension has been studied as a function of diffusion depth. The variation in dimensions (increase in diameter) of all the specimens were observed using an LED-CCD-based non-contact tool. Change in roundness was negligible in all the parts subjected to thermal diffusion treatments (nitriding and boronizing). The specimens subjected to boronizing treatments displayed a consistently large increase in diameter compared to nitriding. The parts of same manufacturing technique and dimensions when subjected to boronizing in a different heat but in same temperature, the change in dimensions were consistent amongst the specimens but different compared to the previous heat. The heats are represented as H1 and H2 in the Figure below.

From the graphs, we could see that the increase in diameter of the specimen is consistently around 20.5 ± 1.5 % for ferrous parts while the increase in diameter for titanium parts are consistently around 25 % in the case of boronizing treatment. However, a significantly lesser change in dimensions were observed in the specimens subjected to nitriding treatment as the

processing temperature was almost half of boronizing temperature. In this research, attempt has been made to understand the dimensional changes that occur post diffusion process; However, there are multiple variables in the process that prevent us from effectively predicting the dimensional changes such as, initial grain size, starting microstructure, manufacturing process, heating rate, temperature, part orientation fixturing, etc. We could use this information to predict the possible change in dimensions post thermal diffusion treatment with certain degree of certainty. With the change in any of the variable could change the dimensional variation, therefore the processing consistency from steel mill to operational table is essential to minimize uncertainty in dimensional variations.

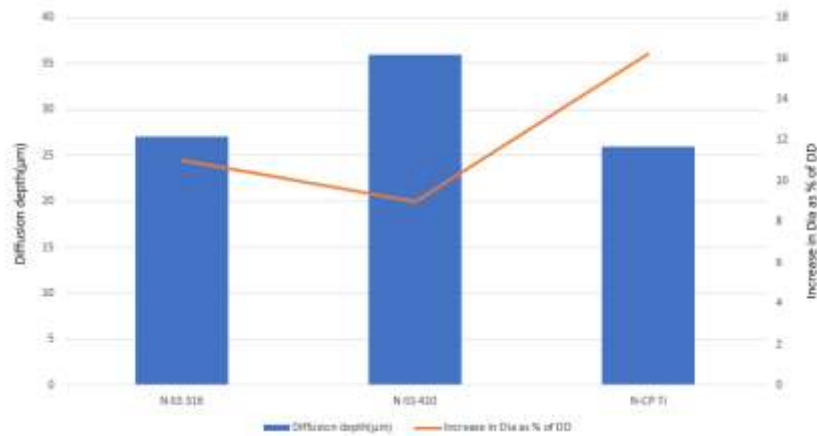


Fig. 5. Diffusion depth and dimensional variation of nitride specimens represented graphically

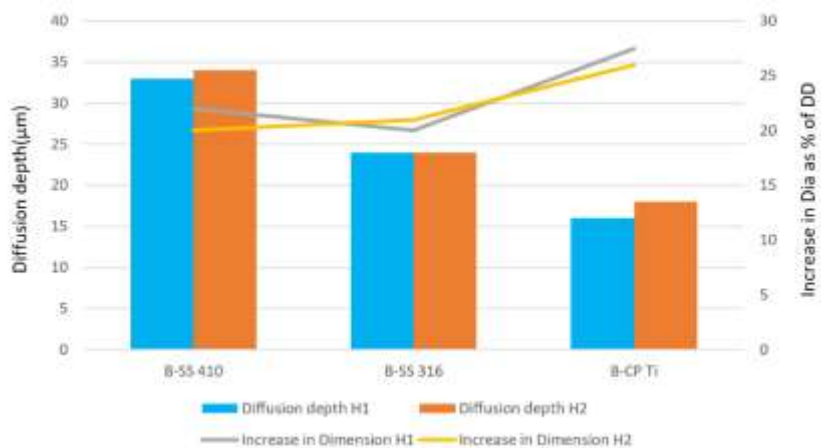


Fig. 6. Diffusion depth and dimensional variation of borided specimens represented graphically

3.4 Metallography

The micro images observed via metallographic investigation using optical microscope are displayed in the Figures 7-9. The images were captured at 500X of optical magnification (10X eye piece and 50X objective) Using stage micrometre and the software coupled with the

microscope we were able to measure the diffusion depth. The diffusion coating depth observed through the optical microscope is reported in the Table 7. The surface of the SS316L specimen subjected to boronizing was observed under SEM (Figure 3.6) before polishing post treatment.

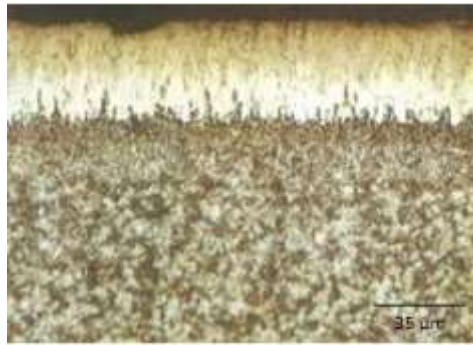


Fig. 7.Micro structure of borided martensitic stainless steel specimen

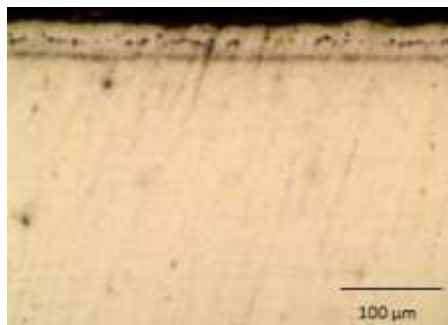


Fig. 8. Microstructure of borided austenitic stainless steel

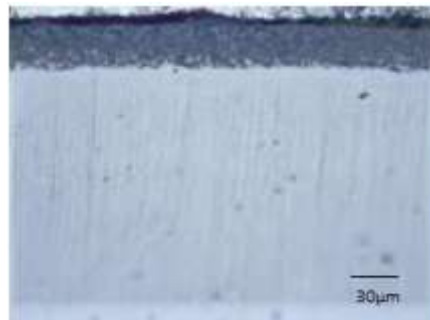


Fig. 9. Microstructure of borided austenitic stainless steel

Specimen ID	Diffusion depth (Average μm)	
Nitrided		
N-SS 316	28	
N-SS 410	36	
N-CP Ti	26	
Borided	Heat 1 (H1) (Average μm)	Heat 2 (H2) (Average μm)
B-SS 316	24	24
B-SS 410	33	34
B-CP Ti	17	19

Fig. 10. Case depth observed in specimens subjected to different thermal diffusion treatments

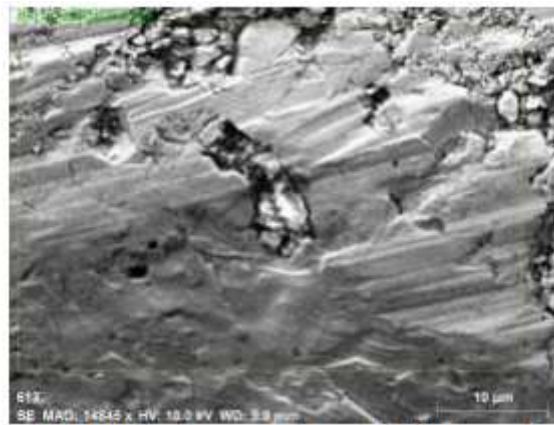


Fig. 11. The surface of SS316L observed through SEM post boronizing of a polished specimen

Both the martensitic and austenitic stainless steel have produced visible diffusion and compound layers, the austenitic stainless (Fig.9.) steel subjected to boronizing has produced a relatively shallow but dense case layer due the higher concentration of alloying elements in the material and consequently a lower case growth rate. A continuous crack travelling parallel to the surface was observed. No similar crack was observed on other specimens of different materials. This crack is expected to be caused due to the presence of a dual phasic boride layer where the rate of thermal expansion coefficient between the layers are different. A presence a residual stresses have caused the crack parallel to the surface. This crack could cause layer delamination and could reduce the service life of the component when used in conditions where the wear debris would be a part of the system and further induce wear in future through various wear mechanisms of 3 body and 2 body systems where the delaminated layer could act as a erodent/abrasive. Therefore it is essential to remove the layer by suitable methods of abrasive grinding or polishing in the case of closed system application. However, in the case of open system application, the presence of a loosely bonded hard layer might not be a significant threat. While the borided martensitic stainless steel SS410 has produced much larger case in comparison, the layer has displayed a characteristic whiskers/dendrites found in low alloys.

3.5 Abrasive Wear

The mechanism of abrasive wear is a complex process as it depends on the reactions of the operating environment. In the three-body abrasion experiment conducted, the increase in surface hardness achieved by subjecting the specimens to boronizing, nitriding and through hardening in the case of AISI 410 has positively impacted the wear characteristics of the material. The boronized specimens of P 410-B group on an average reported a 12.92 times reduction in wear loss compared to untreated stainless materials (410 AM) and 6 times lesser wear loss compared to nitriding (P 410-N). The results of the abrasive wear characterization is reported graphically in the Figure below.

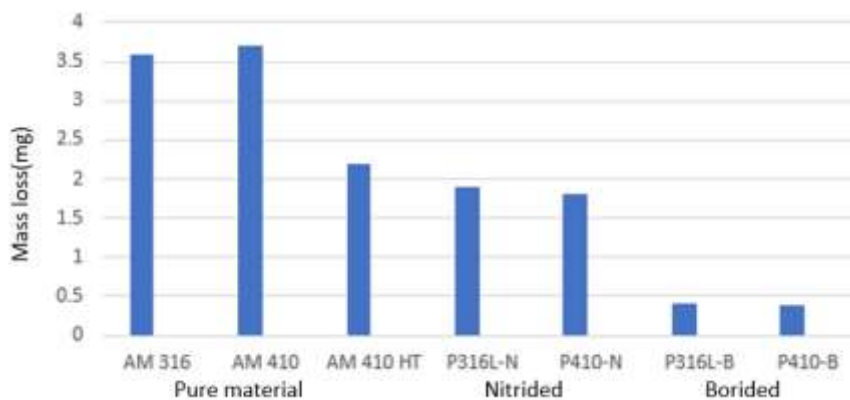


Fig. 12. Graphical representation of mass loss recorded during abrasive wear

The higher surface hardness and layer toughness of the borided materials have benefited the test specimens to resist the ploughing and micro cutting actions. The nitrided materials report only a near 50% reduction in wear losses, this might be attributed towards the lack of the layer's ability to resist the mechanisms of deformation such as micro-cutting or ploughing action commonly associated with three body abrasion.

3.6 Tribologically induced Chemistry Alteration

The surface of hardened and tempered disc of grade AISI 440 was observed under SEM (Figure13.) for any mechanically mixed layers and examined for change in chemistry using an electron diffraction spectroscopy technique. The surface of the disc when examined under EDS, peaks of boron was observed on certain areas of the disc (Figure 18). When we tried to prepare the surface of the disc mechanically to investigate any increase in surface hardness, the patch of material was found to be extremely brittle and displayed very low layer adhesion with the base material. A maximum of 766 HV0.05 was observed on the tribologically modified zone. Since the base material is completely free from boron, the transfer of boron must have happened due to either mechanical mixing or diffusive wear from pin surface to disc surface.

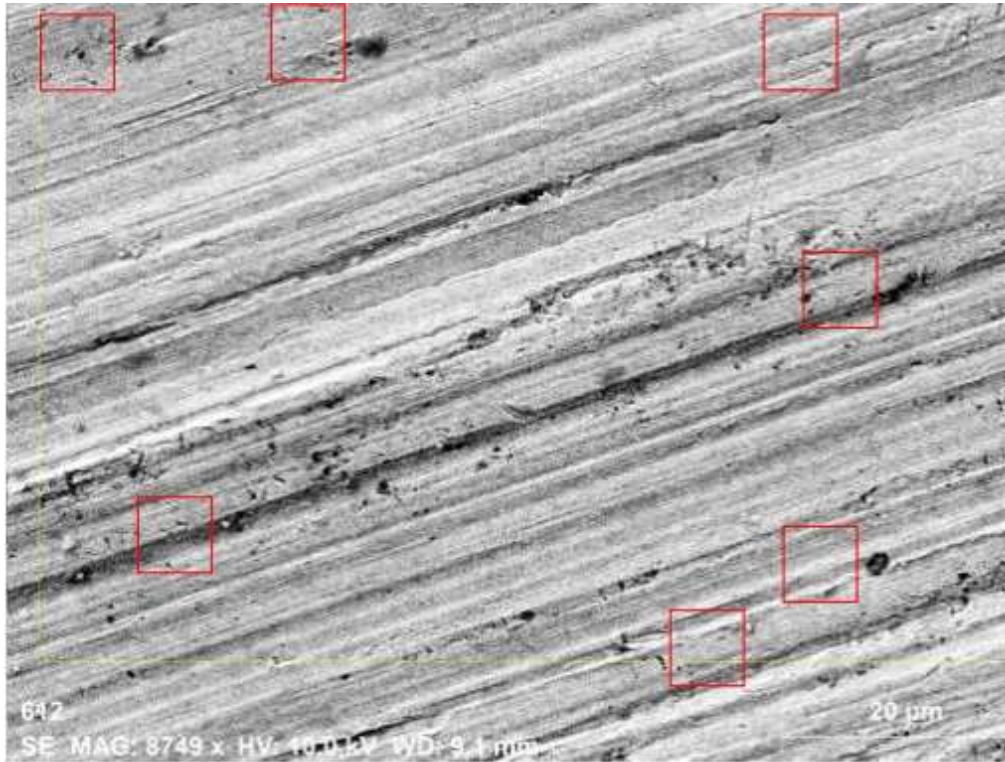


Fig. 13. SEM image of the surface of SS440 disc used against borided specimens with areas of interest enclosed in red squares

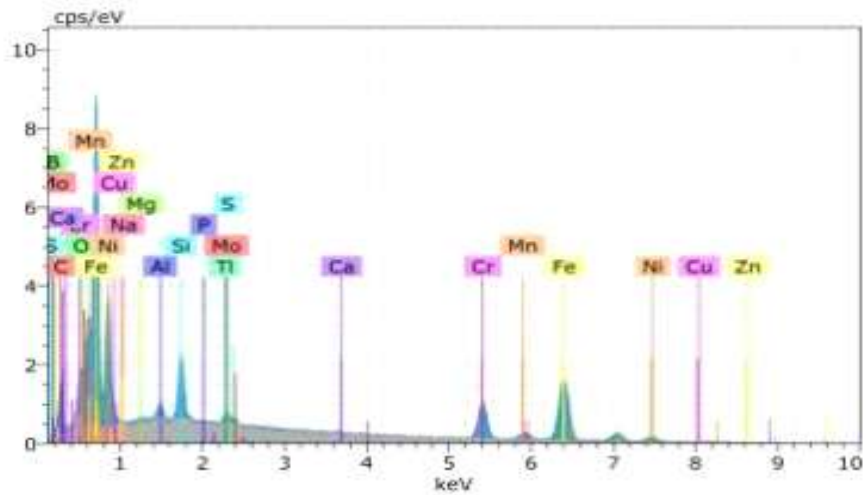


Fig. 14.EDX peaks observed on the worn-out disc indicating the presence of boron in the surface

3.7 Bacterial Sensitivity

The control plates were also prepared with no thermal diffusion processed stainless steel (Figure 15.). These plates with swirl and pour agar/culture mix did not develop any level of bactericidal activity even after 48 hours. This proves that the base material does not process any form of anti-bacterial action. Therefore any ZOI observed on processed specimens would be a result of the thermal diffusion treatments.



Fig. 15. Control plate with no thermal diffusion process (SS316L)

Thermal diffusion treatments have favourably influenced the bacterial sensitivity when tested using pour plate methods. Both, the nitrided and borided specimens created zone of inhibitions thus displaying anti-bacterial activity. These ZOI were too small to measure using ruler, therefore a tool makers' microscope was used to measure the ZOI. The ZOI measured an average of 0.038 mm after one hour of incubation of nitrided specimens. The size of ZOI increased with increase in incubation time, after 48 hour long incubation, the ZOI was visible to naked eye and extended beyond 0.712 mm for the nitrided specimens incubated on the swirl and pour plate. There was no further growth of ZOI with increase in incubation time. The ZOI widths were measured on multiple location and mean width of all the thermal diffusion treated specimens are reported in the Figures 16 and 17.

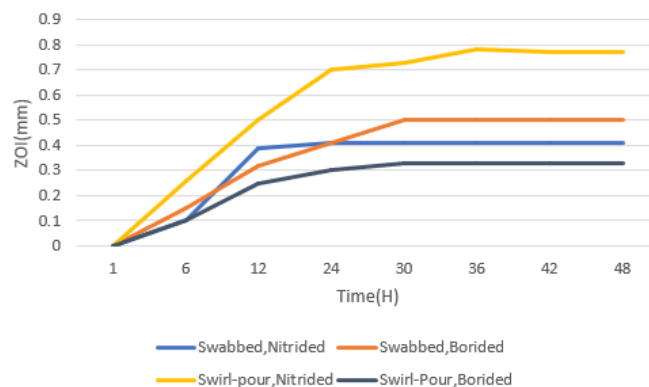


Fig. 16. Measurement of ZOI growth with respect to incubation time for SS316L specimens subjected to different manufacturing techniques

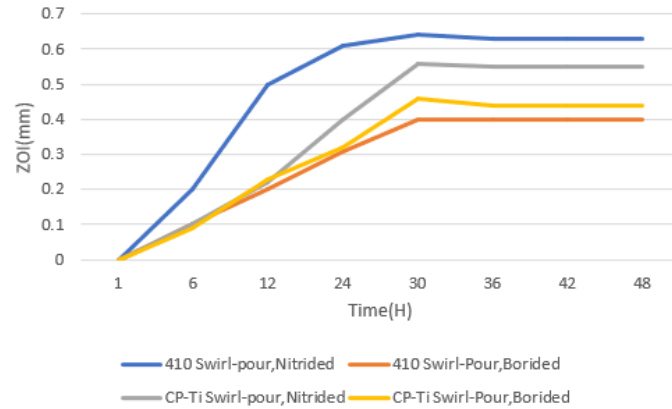


Fig. 17. Measurement of ZOI growth as antibacterial properties of SS410 and CP Ti material subjected to different thermal diffusion treatments and manufactured by polishprocess-polish technique

The short width of ZOI observed is believed to be caused by the relative inertness of the boride and nitride layers (Figures 18-21) when compared to other antibacterial coatings that produce ZOI in order of several millimetre and not fractions of millimetre. A few researchers also found similar test results when studying the antibacterial effects of silver and silver oxide. These materials produced ZOI in the range of 600 μm to 1.1 mm.



Fig. 18. Nitrided SS316L Incubated for 48 hours on swabbed culture



Fig. 19. Borided SS316L incubated on swabbed culture for 48 hours

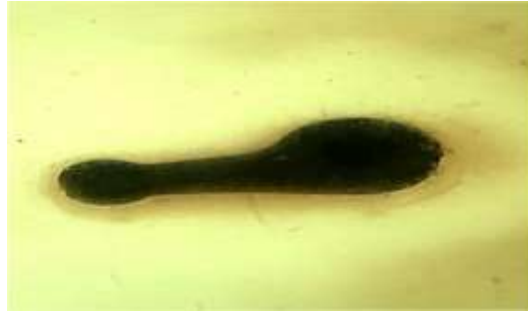


Fig. 20. Nitrided SS316L incubated for 24 h in swirl and pour plate



Fig. 21. Nitrided SS316L incubated for 48 h in swirl and pour plate

4Conclusion

In this research, an attempt was made to study bacterial sensitivity and analyze the antibacterial effects of thermal diffusion treatments. The research also made attempts to study the effect of sliding contact under high applied loads and low moving speeds to simulate human joint movements. Three body abrasive wear tests were conducted on potential medical device materials like SS316L and SS410. The thermal diffusion treatments have positively affected the wear resistance and imparted resilient bactericidal properties. The conclusions of the study are as follows:

Nitriding and boronizing treatments significantly enhance the surface hardness and wear resistance of the base materials, with improvements of up to 4.8 times higher hardness compared to untreated materials. For instance, a maximum surface hardness of 1241 HV0.1 was observed on nitrided austenitic stainless steel (316L), while the unprocessed materials recorded hardness values of 223 HV0.1 for SS410, 157 HV0.1 for SS316L, and 144 HV0.1 for CP Ti.

Thermal diffusion treatments result in predictable increments in dimensions. The increase in diameter is consistently around $20.5 \pm 1.5\%$ for ferrous parts undergoing nitriding, while boronizing treatment causes approximately 25% increase in diameter for titanium parts.

Boronizing demonstrates the highest resistance to wear and tear among the investigated processes. For example, boronized specimens of the P 410-B group show an average reduction in wear loss by 12.92 times compared to untreated stainless materials (410 AM) and 6 times less wear loss compared to nitriding (P 410-N).

Boronizing increases surface roughness, necessitating post-polishing to maintain the desired finish. A maximum roughness reduction of 450% was observed in borided austenitic stainless steel specimens, with an average roughness of 0.64 μm Ra reported on the post-polished specimens.

Both nitriding and boronizing processes exhibit antibacterial activity against *subtilis bacillus* bacteria, providing additional benefits in applications where bacterial growth needs to be minimized.

References

- [1] Kunčická, L., Kocich, R., & Lowe, T.C.: *Progress in Materials Science*, Vol. 88, pp. 232-80 (2017).
- [2] Ho, M., McMillan, A.B., Simard, J.M., Gullapalli, R., & Desai, J.P.: *IEEE Transactions on Robotics*, Vol. 28, pp. 213-22 (2012).
- [3] Petrini, L., & Migliavacca, F.: *Journal of Metallurgy*, Vol. 2011, pp. 1-15 (2011).
- [4] Gunes, I., Erdogan, M., & Çelik, A.G.: *Materials Research*, Vol. 17, pp. 612-18 (2014).
- [5] Lin, K., Li, X., Sun, Y., Luo, X., & Dong, H.: *International Journal of Hydrogen Energy*, Vol. 39, pp. 1-10 (2014).
- [6] Feng, Q., Zhang, D., Xin, C., Liu, X., Lin, W., Zhang, W., & Sun, K.: *Journal of materials science. Materials in medicine*, Vol. 24, pp. 713-24 (2013).
- [7] Groessner-Schreiber, B., Neubert, A., Müller, W.D., Hopp, M., Griepentrog, M., & Lange, K.P.: *Journal of Biomedical Materials Research Part A*, Vol. 64A, pp. 591-99 (2003).
- [8] Pichon, L., Okur, S., Öztürk, O., Rivière, J.P., & Drouet, M.: *Surface and Coatings Technology*, Vol. 204, pp. 2913-18 (2010).
- [9] Feng, Q., Zhang, D., Xin, C., Liu, X., Lin, W., Zhang, W., & Sun, K.: *Journal of materials science. Materials in medicine*, Vol. 24, pp. 713-24 (2013).
- [10] Liguori, G., Antonioli, F., Trombetta, C., Biasotto, M., Amodeo, A., Pomara, G., Belgrano, E.: *Urology*, Vol. 72, pp. 286-89 (2008).
- [11] Wyman, P.: *Coatings for Biomedical Applications*, Vol. 3, pp. 42 (2012).
- [12] Schwartz, C.J., & Bahadur, S.: *Tribology Letters*, Vol. 34, pp. 125-131 (2009).
- [13] Yao, J.Q., Blanchet, T.A., Murphy, D.J., & Laurent, M.P.: *Wear*, Vol. 255, pp. 1113-20 (2003).
- [14] Van de Belt, H., Neut, D., Schenk, W., Van Horn, J.R., Van der Mei, H.C., & Busscher, H.J.: *Acta Orthopaedica Scandinavica*, Vol. 72, pp. 557-71 (2001).
- [15] Sousa, R., & Abreu, M.A.: *Journal of Bone and Joint Infection*, Vol. 3, pp. 108-117 (2018).
- [16] Bafail, A.S., Alamri, A.M., & Spivakovsky, S.: *Evidence-based dentistry*, Vol. 15, pp. 58 (2014).
- [17] Fukagawa, S., Matsuda, S., Miura, H., Okazaki, K., Tashiro, Y., & Iwamoto, Y.: *Journal of Orthopaedic Science*, Vol. 15, pp. 470-76 (2010).
- [18] Van de Belt, H., Neut, D., Schenk, W., Van Horn, J.R., Van der Mei, H.C., & Busscher, H.J.: *Acta Orthopaedica Scandinavica*, Vol. 72, pp. 557-71 (2001).
- [19] Wang, M., & Tang, T.: *Journal of Orthopaedic Translation*, Vol. 17, pp. 42-54 (2019).
- [20] Jaggessar, A., Mathew, A., Wang, H., Tesfamichael, T., Yan, C., & Yarlagaadda, P.K.: *Journal of the Mechanical Behavior of Biomedical Materials*, Vol. 80, pp. 311-19 (2018).